

Alma Mater Studiorum Università di Bologna  
Archivio istituzionale della ricerca

Optimal cruise performance of a conventional helicopter

This is the final peer-reviewed author's accepted manuscript (postprint) of the following publication:

*Published Version:*

Avanzini G., de Angelis E.L., Giulietti F. (2021). Optimal cruise performance of a conventional helicopter. PROCEEDINGS OF THE INSTITUTION OF MECHANICAL ENGINEERS. PART G, JOURNAL OF AEROSPACE ENGINEERING, 0(0), 1-14 [10.1177/09544100211024091].

*Availability:*

This version is available at: <https://hdl.handle.net/11585/856658> since: 2022-02-11

*Published:*

DOI: <http://doi.org/10.1177/09544100211024091>

*Terms of use:*

Some rights reserved. The terms and conditions for the reuse of this version of the manuscript are specified in the publishing policy. For all terms of use and more information see the publisher's website.

This item was downloaded from IRIS Università di Bologna (<https://cris.unibo.it/>).  
When citing, please refer to the published version.

(Article begins on next page)

This is the final peer-reviewed accepted manuscript of:

**Avanzini G., de Angelis E.L., Giulietti F., Optimal cruise performance of a conventional helicopter, Proceedings of the Institution of Mechanical Engineers (2022), Part G: Journal of Aerospace Engineering, 236 (5), pp. 865 - 878, DOI: 10.1177/09544100211024091**

The final published version is available online at:

<https://journals.sagepub.com/doi/10.1177/09544100211024091>

Rights / License:

The terms and conditions for the reuse of this version of the manuscript are specified in the publishing policy. For all terms of use and more information see the publisher's website.

*This item was downloaded from IRIS Università di Bologna (<https://cris.unibo.it/>)*

***When citing, please refer to the published version.***

---

# Optimal Cruise Performance of a Conventional Helicopter

Giulio Avanzini<sup>1</sup>, Emanuele L de Angelis<sup>2</sup> and Fabrizio Giulietti<sup>2</sup>

## Abstract

This paper presents an analytical framework for investigating the cruise performance of conventional helicopter configurations. Starting from the analysis of power required in straight and level flight, endurance and range performance of turbine- and battery-powered rotorcraft are considered, for which it is assumed that fuel consumption and constant-power battery discharge models are respectively made available. The original contributions of the paper are represented by (a) a closed-form formulation for expected endurance and range for both classes of vehicles, where electrical helicopters have not been dealt with in previous studies; (b) the analytical derivation of an accurate estimate for best endurance and best range airspeeds as a function of relevant system parameters. The approach is validated by analyzing two reference helicopters, showing good physical insight and better accuracy with respect to other techniques available in the literature, for the identification of an energy-efficient cruise flight strategy.

## Keywords

helicopter performance, endurance, range, best range speed, electric rotorcraft

## Introduction

The distance and time flown by a fixed-wing aircraft burning a certain amount of fuel can be analytically determined on the basis of the well known Breguet range and endurance equations.<sup>1,2</sup> Assuming that thrust specific fuel consumption (for turbine-powered aircraft) or horsepower specific fuel consumption (for piston-props) is known and (at least approximately) independent of the flight condition (airspeed and altitude), it is possible to easily identify the best range and best endurance airspeeds, that is, the flight conditions which maximize cruise performance. Only a few aircraft parameters are required, namely parabolic drag polar coefficients, wing loading, specific fuel consumption, and propeller efficiency (if a propeller is present). Aircraft weight reduction during cruise is accounted for, typically resulting in different cruise strategies.<sup>3</sup> Conversely, the analysis of performance for battery-powered aircraft represents a relatively recent topic of discussion in the community.<sup>4,5</sup> Weight is constant during cruise and attention is required for the mathematical modeling of the battery discharge process.<sup>6</sup>

In recent literature, a great deal of interest was devoted to the analysis and improvement of rotorcraft performance by reducing required power.<sup>7</sup> Different solutions were considered, such as rotor power reduction by means of variable rotor rate and dynamic twist,<sup>8</sup> blade extendable chord,<sup>9</sup> or by reducing parasite power or interference between configuration elements.<sup>10,11</sup> In particular, variable-speed rotor studies represent a promising research field for rotorcraft performance improvement, fuel-consumption reduction, and engine emissions abatement. As a matter of fact, the problems related to employing main rotor variable speed are numerous, and an interdisciplinary approach is typically required for successfully tackling the resulting optimization problem.<sup>12</sup>

The effect of structural and aerodynamic uncertainties on the prediction of required power was investigated by Siva et al.,<sup>13</sup> where an aerodynamic model based on blade element and momentum theory was used to predict helicopter performance. Relevant main rotor parameters, such as blade chord, rotor radius, airfoil lift-curve slope, blade profile drag coefficient, rotor angular velocity, blade pitch angle, and blade twist are considered as random variables. The propagation of these uncertainties to performance parameters, such as thrust and power coefficients, are then studied using Monte Carlo simulations.

If on one side most studies typically focus on a single flight phase, on the other hand a few attempts have also been made to outline a multiphase formulation. A multi-engine helicopter sustaining a single engine failure provides such an example, where the sudden reduction of available power following the loss of one engine divides the maneuver into two phases, before and after the failure. Such a scenario is considered by Visser,<sup>14</sup> where an optimal solution for a take-off maneuver is derived, during which all engines are operating, and the best possible compromise between the requirements related to a rejected take-off and a continued take-off flight maneuver after failure is identified, for any given engine failure time.

Unmanned aerial vehicles (UAVs), particularly small battery-powered helicopters, are gaining interest from

---

<sup>1</sup>University of Salento, Department of Engineering for Innovation (DII), Italy

<sup>2</sup>University of Bologna, Department of Industrial Engineering (DIN), Italy

## Corresponding author:

Emanuele Luigi de Angelis, University of Bologna, Department of Industrial Engineering (DIN), Via Fontanelle 40, 47121 Forlì, Italy  
Email: emanuele.deangelis4@unibo.it

worldwide researchers due to their various advantages, such as small size, light weight, and low cost. Demand for these capabilities has increased, in both military and civil applications, increasing the interest on research aimed at deriving tools for optimal sizing procedures, accurate dynamic models, and automated control systems.<sup>15,16</sup> A novel approach for the robust design of a small-scale unmanned helicopter was presented by Abhiram et al.<sup>17</sup> for efficient hover performance, which was predicted using a numerical implementation of a refined blade element momentum theory. Taguchi method was shown to provide a robust design solution characterized by a significant reduction in the power required to hover (when compared to a baseline helicopter design of similar size and configuration).<sup>18</sup> With respect to the analysis of power requirements and the determination of flight endurance for a helicopter in hover, preliminary experimental results were also obtained for a small-scale autonomous platform designed for Martian exploration.<sup>19</sup> In such a case, a unique set of design challenges was addressed, with severe constraints posed by a low-Reynolds-number, high-Mach-number flow condition on the rotor blades.

To the best of the authors' knowledge, little attention was paid to estimate of global endurance and range performance of a helicopter as a function of system parameters, especially in terms of an analytical approach similar to that which has been available in the fixed-wing aircraft case for almost a century. Only crude approximations are available for rotorcraft, even for the case of conventional, single main rotor helicopters, which represent the most widely used class of rotorcraft in civil applications.<sup>20,21</sup> The objective of the present paper is thus to fill this gap, by deriving an analytical framework that allows for a physically consistent and reasonably accurate estimate of helicopter cruise performance, on the basis of a limited number of information on the configuration and its powerplant. The formulas derived for range and endurance immediately provide a valuable instrument for performance analysis, but it may be used also for preliminary helicopter sizing, when vehicle design process is at an early conceptual stage.

The total power required in steady rectilinear level flight is derived first, following the method presented by McCormick.<sup>22</sup> Analytical expressions for specific endurance and specific range are then obtained, on the basis of a simple expression of fuel consumption (for turbine-driven helicopters), or a constant-power battery-discharge model (for electrically driven rotorcraft). A few simplifying assumptions, that will be carefully analyzed, are introduced for deriving closed-form expressions of range and endurance, together with the airspeed which maximizes each one of them.

The derivation of a fully analytical approach based on physical characteristics of the airframe (rotor geometry, blade airfoil aerodynamic characteristics, vehicle weight, and fuselage drag coefficients) represents the major contribution of the paper, with respect to previous techniques available in the literature. As an example, Johnson<sup>20</sup> provides two rough estimates of helicopter performance. In the first case, average values of specific range and endurance at an intermediate weight between initial and final weights are derived, which are then multiplied by

the amount of fuel burned, under the assumption that the total fuel weight is a small fraction of gross weight. A similar derivation is also proposed by Leishman,<sup>21</sup> where the limitation represented by the assumption of small fuel fractions is stressed. The second, slightly more accurate, approach proposed by Johnson is based on the derivation of a Breguet-like equation, assuming that the specific fuel consumption is independent of power delivered by the engine and, as major approximations, rotor thrust equals weight and the power-to-thrust ratio is independent of weight. In the derivations discussed in the present paper, the variation of specific fuel consumption and, more importantly, rotor blade profile power are instead accounted for, together with system power, which may play a relevant role in modern fly-by-wire helicopters or unmanned vehicles with power-demanding payloads.

As a further contribution, relevant for applications dealing with electrically driven rotorcraft, a fully electric propulsion system is also analyzed, where endurance and range performance depends on the battery discharge process. To this aim, a recent constant power discharge model is considered, valid for several types of batteries.<sup>6</sup> For each class of vehicles, equipped with either a thermal engine or a fully electric power system, an applicative example is considered, which demonstrates the validity of the modeling approach and of the simplifying assumptions adopted to obtain closed-form, analytical results. A comparison with the methods described by Johnson<sup>20</sup> and Leishman<sup>21</sup> highlights the improvements in terms of accuracy for 1) the estimate of endurance and range performance at various airspeeds and 2) the evaluation of optimal velocities which maximize both of them.

In what follows, the next section recalls the most relevant features of the model presented by McCormick<sup>22</sup> for the determination of power required by a conventional single main rotor helicopter in forward flight, as a function of airspeed. In Section 3, the framework for the analysis of range and endurance performance of conventional, single main rotor helicopters is derived, which is then applied to two relevant configurations in Section 4. A section of concluding remarks summarizes the findings of this paper.

## Power Required for Cruise Flight

The power required by a helicopter in steady-level flight,

$$P_r = P_p + P_{mr} + P_{tr} + P_s$$

is expressed as the sum of four contributions,<sup>22</sup> namely parasite power  $P_p$ , main and tail rotor power,  $P_{mr}$  and  $P_{tr}$ , and power required by on-board systems  $P_s$ . Parasite power is due to fuselage drag,  $D$ , and it is equal to  $P_p = DV = 0.5 \rho f V^3$ , where  $\rho$  is air density and  $f$  is referred to as fuselage equivalent flat plate parasitic area. Power required by on-board systems,  $P_s$ , is assumed to be approximately constant. Main rotor power,  $P_{mr}$ , is the sum of induced and rotor blade profile power:

$$P_{mr} = P_{ind} + P_{pr} \quad (1)$$

Induced power is given by  $P_{ind} = \xi P_{id}$ , where the ideal power  $P_{id} = T v_i$  is determined on the basis of momentum

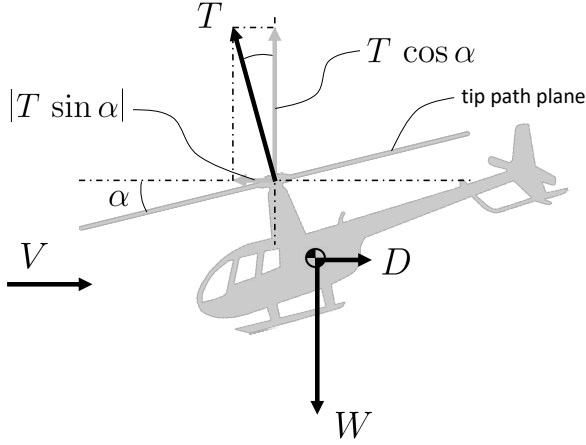


**Figure 1.** Side view of rotorcraft platform.

theory applied to an actuator disk as the product of rotor thrust,  $T$ , and induced speed,  $v_i$ . The empirical coefficient  $\xi$  accounts for a multitude of aerodynamic dissipation effects, including blade tip losses and nonuniform inflow, which are not detailed in the present formulation. The value of  $\xi$  is not necessarily assumed independent of advance ratio, but the use of a mean value in the range between 1.15 and 1.25 is usually sufficient accurate for preliminary predictions of power requirements.<sup>21</sup> For the aim of the present analysis, the vertical drag produced by the main rotor downwash on the fuselage and appendages is also disregarded. According to Glauert's hypothesis, the induced velocity and main rotor thrust are related by the following equation:<sup>20</sup>

$$v_i = T / (2 \rho A V_D) \quad (2)$$

where

$$V_D = \sqrt{(v_i - V \sin \alpha)^2 + (V \cos \alpha)^2} \quad (3)$$

is the flow velocity at rotor disc and  $\alpha$  is the angle of attack of the rotor plane, assumed positive when air impinges on rotor disc from below (see Fig. 1). Let  $W = Mg$  be the gross weight of the aircraft, where  $M$  is the mass and  $g$  is the gravitational acceleration. In steady level flight the sum of forces acting on the rotorcraft in the direction of flight and along the local vertical provide the equilibrium conditions

$$D + T \sin \alpha = 0 ; \quad W - T \cos \alpha = 0 \quad (4)$$

Thrust required to maintain a steady-level flight at the given velocity  $V$  results from equation (4), such that

$$T = \sqrt{W^2 + D^2} \quad (5)$$

Let  $A = \pi R^2$  be the main rotor disc area, where  $R$  is the rotor radius. When a hovering condition is analyzed, such that  $V = 0$ ,  $D = 0$ , and  $T = W$ , a closed-form expression is obtained for the induced velocity from equation (2), namely  $v_i = v_{i0} = \sqrt{W / (2 \rho A)}$ . In the most general case, an iterative scheme is required for equation (2), which typically converges after a few iterations, such as a simple fixed-point algorithm or a Newton-Raphson approach.<sup>21</sup>

Profile power  $P_{pr}$  is obtained from blade element theory in the form:

$$P_{pr} = \rho A V_T^3 C_{p_{pr}} \quad (6)$$

where  $V_T = \Omega R$  is the blade tip speed and  $\Omega$  is the rotor angular rate, assumed to be a constant. Let  $\sigma = N_b c / (\pi R)$  be the rotor solidity, where  $N_b$  is the number of main rotor blades and  $c$  is rotor blade mean chord. The profile power coefficient, which includes the effects of radial and reverse flow losses, is written as<sup>21</sup>

$$C_{p_{pr}} = \frac{\sigma \bar{C}_d}{8} \left( 1 + 4 \mu^2 + \frac{5}{8} \mu^4 \right) + \Delta C_{p_{pr}} \quad (7)$$

where  $\bar{C}_d$  is blade airfoil average drag coefficient,  $\mu = V / V_T$  is the advance ratio, and  $\Delta C_{p_{pr}}$  is the extra rotor profile power determined by compressibility effects on the advancing blade. The average drag coefficient is a quadratic function of the average blade lift coefficient  $\bar{C}_l$ , namely

$$\bar{C}_d = C_{d0} + k \bar{C}_l^2 \quad (8)$$

where  $C_{d0} > 0$ ,  $k > 0$ , and

$$\bar{C}_l = 6 C_T / \left[ \sigma \left( 1 + \frac{3}{2} \mu^2 \right) \right] \quad (9)$$

is related to the thrust coefficient  $C_T = T / (\rho A V_T^2)$ . Compressibility effects are approximated by Johnson<sup>21</sup> as:

$$\frac{\Delta C_{p_{pr}}}{\sigma} = \begin{cases} m_1 (\Delta M_b) + m_2 (\Delta M_b)^2 & \text{for } M_b \geq M_{dd} \\ 0 & \text{for } M_b < M_{dd} \end{cases} \quad (10)$$

where  $m_1 = 0.007$  and  $m_2 = 0.052$  are model coefficients and  $\Delta M_b$  is the amount the advancing blade tip Mach number  $M_b$  exceeds the drag divergence Mach number  $M_{dd}$  of the airfoil section, that is  $\Delta M_b = M_b - M_{dd}$ . In the present case, it is  $M_b = (V + V_T) / a$ , where  $a$  is the speed of sound, and  $M_{dd}$  is obtained from tests on 2D blade airfoil.

Tail rotor power is obtained by the same identical approach followed for the main rotor induced and profile power components. In a simplified scenario, the tail rotor thrust magnitude  $T_{tr}$  is derived by imposing the equilibrium condition for rotational motion about the aircraft yaw axis. Let  $l_{tr}$  be the length of the lever arm of tail rotor thrust vector with respect to the yaw-axis, considered to pass through the rotorcraft center of gravity. The required tail rotor thrust will be  $T_{tr} = (P_p + P_{mr}) / (\Omega l_{tr})$ . This assumes that there is no off-loading of the tail rotor by the vertical fin. Also, the interference between the main rotor and the tail rotor, and between the tail rotor and the vertical fin, is neglected in this preliminary analysis.

## Performance analysis and optimization

In the present Section, performance analysis and optimization in forward flight are addressed for both turbine and battery-powered conventional helicopter configurations.

### Turbine-powered helicopter

In case of internal combustion powerplant, the larger part of the available turbine shaft power,  $P_{sh}$ , is delivered to the main rotor and the tail rotor by means of dedicated transmission systems. Power losses are taken into account by  $\eta_{mr}$ , and  $\eta_{tr}$  parameters. They represent main and tail rotor efficiency, respectively, and they are assumed to be

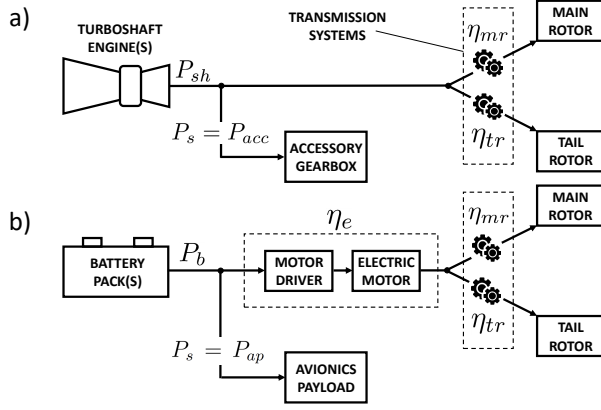


**Figure 2.** Powerplant systems for conventional a) turbine-powered and b) battery-powered single main rotor helicopters.

approximately constant. The remaining part of the available power,  $P_{acc}$ , supplies accessory subsystems (fuel and oil pumps, electrical generators, and other auxiliary services) (see Fig. 2.a). By imposing a steady level flight condition, required and available power balance equation provides:

$$P_{sh} = (P_{mr} + P_p) / \eta_{mr} + P_{tr} / \eta_{tr} + P_{acc} \quad (11)$$

Steady level flight performance analysis of a turbine-powered helicopter, intended as endurance and range evaluation, requires the specific fuel consumption model to be a function of the delivered shaft power. Starting from the analysis presented by Stepniewski and Keys,<sup>23</sup> a model of general validity is derived by Leishman,<sup>21</sup> which can be easily adapted to represent the case of reciprocating engines, where the fuel flow required by a turboshaft engine for delivering the shaft power  $P_{sh}$  determines a decrease of rotorcraft weight given by  $dW/dt = -BSFC P_{sh}$ , provided  $BSFC(P_{sh}) = c_0/P_{sh} + c_1$  is the Brake Specific Fuel Consumption. In particular, it is  $c_0 = N_e \delta \sqrt{\theta} \bar{c}_0$ , where  $N_e$  is the number of operative engines,  $\delta$  and  $\theta$  respectively represent the atmospheric pressure ratio and the temperature ratio at the considered altitude, while  $\bar{c}_0$  and  $c_1$  are positive coefficients that characterize the particular engine. It is finally assumed, for simplicity, that engine performance is not affected by forward speed and that the residual thrust provided by the exhaust of turbine hot gases can be disregarded. According to the previous definition, one obtains:

$$dt/dW = -1/(BSFC P_{sh}) = -1/(c_0 + c_1 P_{sh}) \quad (12)$$

such that the Best Specific Endurance (BSE) condition is easily found at the minimum shaft power speed,  $V_{P_{min}}$ , which is a well known result in the field of helicopter performance optimization.<sup>21</sup> This condition can be obtained either graphically on the plot of equation (11) or numerically by means of a search algorithm, such as the parabolic search or the simplex method.<sup>24,25</sup> An analytical expression of  $V_{P_{min}}$ , which represents the optimum speed to fly at minimum auto-rotation rate of descent or maximum rate of climb, is derived by imposing  $\partial P_{sh}/\partial V = 0$ . Because of the presence of a correction term,  $\Delta C_{p_{pr}}$  from equation (10), related to rotor parasite power increment due

to compressibility effects, the expression of  $\partial P_{sh}/\partial V$  is only piecewise continuous. Provided that the minimum power condition is expected to lie well outside of the speed range where compressibility effects become significant, this aspect is not relevant in this framework.

The analytical expression of  $V_{P_{min}}$  becomes available after introducing the following assumptions:

**Assumption 1.** For sufficiently high forward speeds, the main rotor induced velocity  $v_i$  becomes small if compared to  $V$ . Hence,  $v_i \approx T/(2\rho AV)$ .<sup>22</sup>

**Assumption 2.** Tail rotor power is neglected,<sup>21</sup>  $P_{tr} \approx 0$ .

**Assumption 3.** The main rotor profile power builds slowly with airspeed,  $\partial P_{pr}/\partial V \approx 0$ , provided that  $M_b \leq M_{dd}$ . From equations (6)-(10), the (almost) constant value of  $P_{pr}$  is evaluated at hover, where:

$$P_{pr} \approx P_{pr_0} = \frac{\rho^2 \sigma^2 A^2 V_T^4 C_{d_0} + 36 k W^2}{8 \rho \sigma A V_T}$$

**Assumption 4.** It is assumed that  $\xi f/(4A) \ll 1$ , which holds for most practical applications.

Following Assumptions 1-3, the minimum power condition only depends on variation in main rotor induced power and parasitic power, provided the power delivered to the accessory subsystems,  $P_{acc}$ , is a constant. Then, imposing  $\partial P_{sh}/\partial V = 0$  yields:

$$3 f \rho^2 [1 + \xi f/(4A)] V^4 - \xi W^2/A = 0 \quad (13)$$

By considering Assumption 4, the following approximation for BSE airspeed is finally found:<sup>21</sup>

$$V_{BSE} = \sqrt{\frac{W}{2\rho A}} \sqrt[4]{\frac{4\xi}{3f/A}} = v_{i0} \sqrt[4]{\frac{4\xi}{3f/A}} \quad (14)$$

which increases with increasing density altitude and disk loading.

Helicopter endurance in straight and level flight at a given constant airspeed  $V$  is calculated by numerical integration of specific endurance in equation (12), expressed as a function of  $W$ , between initial cruise weight,  $W_i$ , and final weight,  $W_f = W_i - W_{fuel}$ , provided  $W_{fuel}$  is the fuel weight burned during the cruise flight. Taking into account Assumptions 1, 2, and 4, a closed-form expression that approximates the exact endurance is obtained, introducing the following additional hypothesis:

**Assumption 5.** For a given cruise speed, the main rotor profile is poorly affected by weight variation due to fuel consumption,  $\partial P_{pr}/\partial W \approx 0$ . By taking into account equations (6)-(10), the value of  $P_{pr}$  is evaluated in the initial cruise condition,  $P_{pr} \approx P_{pr_i} = P_{pr}(W = W_i)$ .

The integration of the specific endurance in equation (12) under the above mentioned hypotheses gives:

$$t = [\eta_{mr}/(\phi\psi)] [\arctan(\phi W_i/\psi) - \arctan(\phi W_f/\psi)] \quad (15)$$

where

$$\phi = \sqrt{\xi c_1/(2\rho AV)} \quad (16)$$



and

$$\psi = \sqrt{c_0 \eta_{mr} + c_1 (P_{pr_i} + \eta_{mr} P_{acc} + \rho f V^3/2)} \quad (17)$$

are a function of speed  $V$ . Note from equations (6)-(10) that, for a given speed, the constant value  $P_{pr_i}$  represents an upper bound to the main rotor profile power  $P_{pr}$  along the cruise. This allows to partially compensate the omission of tail rotor power in Assumption 2 from the analytical computation of performance indices.

The specific range of a turbine-powered helicopter is obtained by multiplying the specific endurance in equation (12) by the airspeed  $V$ , namely

$$dx/dW = -V/(BSFC P_{sh}) = -V/(c_0 + c_1 P_{sh}) \quad (18)$$

By taking into account Assumptions 1-4 and approximating the BSFC as a constant value, not dependent on  $P_{sh}$ , a closed-form solution for the Best Specific Range (BSR) airspeed is obtained by setting to zero the derivative of equation (18) with respect to  $V$ . This leads to:

$$a_4 V^4 + a_1 V + a_0 = 0 \quad (19)$$

where the polynomial coefficients are  $a_4 = f \rho^2$ ,  $a_1 = -\rho (P_{pr_0} + \eta_{mr} P_{acc})$ , and  $a_0 = -\xi W^2/A$ . Let

$$\Delta_0 = -12 a_4 a_0; \quad \Delta_1 = 27 a_4 a_1^2 \quad (20)$$

and

$$L = \sqrt[3]{\frac{\Delta_1 + \sqrt{\Delta_1^2 - 4 \Delta_0^3}}{2}} \quad (21)$$

$$M = \frac{1}{2} \sqrt{\frac{1}{3 a_4} \left( L + \frac{\Delta_0}{L} \right)}$$

It is possible to prove that the fourth order polynomial in equation (19) always has one pair of complex conjugate roots. One of the remaining real solutions is negative. The only real positive solution provides the value of the BSR airspeed in the form:<sup>26</sup>

$$V_{BSR} = M + \frac{1}{2} \sqrt{-4M^2 - \frac{a_1}{M a_4}} \quad (22)$$

**Remark 1.** Assumption 3, which implies that rotor profile power is considered as approximately constant, allows one to drop the (discontinuous) contribution to  $C_{p_{pr}}$  due to compressibility effects at high speed. As a matter of fact, the best specific range airspeed is expected to lie either below or close to the lower boundaries of this region, thus causing a limited error on the validity of the analytical solution for  $V_{BSR}$  derived above (see equation (22)) with respect to its actual value. The latter can nonetheless be graphically determined. This aspect will be analyzed in quantitative terms in the next Section.

**Remark 2.** Although equation (22) provides the exact solution to the fourth order polynomial in equation (19), a more compact yet approximate expression can be envisaged. To this aim, note that the considered quartic equation can be written in perturbed form as:<sup>27</sup>

$$\epsilon h(V) = g(V) \quad (23)$$

where

$$g(V) = f \rho^2 V^4 - \xi W^2/A$$

and

$$h(V) = \rho (P_{pr_0} + \eta_{mr} P_{acc}) V$$

are a function of airspeed  $V$  and  $\epsilon$  is an artificial perturbation term, equal to 1 in the complete polynomial in equation (19). The exact solutions of the perturbed problem is expressed in terms of a regular perturbation series, in the form

$$V = V_0 + \epsilon V_1 + \epsilon^2 V_2 + \epsilon^3 V_3 + \dots \quad (24)$$

where the  $\epsilon^k V_k$  functions, defined for  $k = 1, \dots, +\infty$  define the asymptotic ordering of terms,  $1 \gg \epsilon V_1 \gg \epsilon^2 V_2 \gg \epsilon^3 V_3 \gg \dots$  as  $\epsilon \rightarrow 0$ . The considered problem also introduces the leading-order term  $V_0$  as the asymptotic approximation to the exact solution for  $\epsilon \rightarrow 0$ , with the higher order terms in the expansions being considered as successively smaller corrections to  $V_0$  in that limit. The leading-order problem is evaluated at the limit value  $\epsilon = 0$ , namely  $g(V_0) = 0$ , yielding four different solutions. The only real positive root is given by

$$V_0 = \sqrt{\frac{W}{2 \rho A}} \sqrt[4]{\frac{4 \xi}{f/A}} = v_{i0} \sqrt[4]{\frac{4 \xi}{f/A}} \quad (25)$$

The zeroth-order solution coincides with the approximate value of the BSR airspeed provided by Leishman,<sup>21</sup> where the contribution due to main rotor profile power is neglected and the BSFC is assumed to be a constant, not dependent on  $V$ . In such a framework, the BSR airspeed was found by simply minimizing the ratio  $P_{sh}/V$ , provided that only main rotor induced and parasitic power are accounted for. Substituting the regular perturbation series defined by equation (24) into equation (23) and equating the coefficients of  $\epsilon$ -terms with the same degree, allow one to obtain a set of equations where all  $V_k$  functions are uniquely defined. In the present framework, an approximate solution is sought by truncating the considered series at the term with  $k = 2$ , such that  $V \approx V_0 + \epsilon V_1 + \epsilon^2 V_2$ . It is straightforward to obtain

$$V_1 = \frac{P_{pr_0} + \eta_{mr} P_{acc}}{4 f \rho V_0^2} \quad (26)$$

and

$$V_2 = -V_1^2 / (2 V_0) \quad (27)$$

with the result that, after restoring the artificial perturbation parameter to 1, the approximate second-order BSR airspeed becomes:

$$V_{BSR} = V_0 \left[ 1 + \frac{P_{pr_0} + \eta_{mr} P_{acc}}{4 f \rho V_0^3} - \frac{(P_{pr_0} + \eta_{mr} P_{acc})^2}{2 V_0^2} \right] \quad (28)$$

As a final contribution, the range of a turbine-powered helicopter during a constant speed cruise is obtained by multiplying the endurance  $t$  in equation (15) by the airspeed  $V$ , such that

$$x = [\eta_{mr} V / (\phi \psi)] [\arctan(\phi W_i / \psi) - \arctan(\phi W_f / \psi)] \quad (29)$$

### Battery-powered electric helicopter

In the case of battery-powered helicopters, typically represented by small-scale remotely piloted rotorcraft, the power generated by the battery pack,  $P_b$ , is first reduced by an amount equal to  $P_s = P_{ap}$ , which represents the total power required for avionics and possible payload. The net power is then reduced by losses within the electric driving system made of a speed regulator and the electric motor(s) by the efficiency  $\eta_e$  (see Fig. 2.b), assumed to be approximately constant. In the end, the available shaft power is distributed to the main and tail rotor by the above mentioned transmission system. The total power requested from the battery packs for cruise flight thus becomes:

$$P_b = (P_{mr} + P_p) / (\eta_e \eta_{mr}) + P_{tr} / (\eta_e \eta_{tr}) + P_{ap} \quad (30)$$

where  $P_{ap}$  is the power delivered to avionics and payload systems. It can be noted that, for a helicopter in a steady speed condition with a given gross weight  $W$ , the battery power  $P_b$  is a constant. In the work by Avanzini et al.<sup>6</sup> a novel formulation for constant-power battery discharge process is proposed, where discharge time  $t$  is expressed as a function of discharged capacity and absorbed power. Let  $I = I(t)$  be the current provided by the battery pack and  $C = C(t)$  be the discharged capacity at time  $t$ , obtained as

$$C(t) = \int_0^t I(s) ds \quad (31)$$

Assuming  $P_b > 0$ , discharge time is expressed in the form

$$t = \lambda P_b^\gamma C^\beta = \lambda [(P_{mr} + P_p) / (\eta_e \eta_{mr}) + P_{tr} / (\eta_e \eta_{tr}) + P_{ap}]^\gamma C^\beta \quad (32)$$

where coefficients  $\lambda > 0$ ,  $\gamma < -1$ , and  $0 < \beta < 1$ , determined experimentally at the given ambient temperature, depend on battery technology, aging, and pack configuration.

It is clear from equation (32) that best endurance condition is obtained by flying at the minimum required battery power speed. Taking into account Assumptions 1-4, provided  $P_{ap}$  is a constant, it follows that the minimum battery power condition can be thus determined by the variation in main rotor induced power and parasitic power, such that the corresponding approximate value of airspeed is still indicated by equation (14).

The range of an electrically-driven helicopter is obtained by multiplying the endurance  $t$  in equation (32) by the airspeed  $V$ , namely

$$x = \lambda V P_b^\gamma C^\beta = \lambda V [(P_{mr} + P_p) / (\eta_e \eta_{mr}) + P_{tr} / (\eta_e \eta_{tr}) + P_{ap}]^\gamma C^\beta \quad (33)$$

The optimal value for the best range airspeed is obtained by equating to zero the derivative of range  $x$  in equation (33) with respect to  $V$ . Taking into account Assumptions 1-4, this yields:

$$f \rho^2 (1 + 3\gamma) V^4 + 2 \rho (P_{pr_0} + \eta_e \eta_{mr} P_{ap}) V - \xi (\gamma - 1) W^2 / A = 0 \quad (34)$$

The fourth order polynomial in equation (34) has the same structure of equation (19), provided the constant

coefficients are now given by  $a_4 = f \rho^2 (1 + 3\gamma)$ ,  $a_1 = 2 \rho (P_{pr_0} + \eta_e \eta_{mr} P_{ap})$ , and  $a_0 = -\xi (\gamma - 1) W^2 / A$ . It is easy to prove that equation (34), which can be numerically solved, provides one pair of complex conjugate roots and only one real positive solution is available, corresponding to the best range airspeed, in the same form introduced in equations (20)-(22).

**Remark 3.** Although an analytical solution to the fourth order polynomial in equation (34) is available, an approximate expression can be evaluated, with a procedure similar to that already discussed in the case of turbine-powered helicopters. To this aim, the considered quartic equation is written in perturbed form as  $\epsilon h(V) = g(V)$ , where  $g(V) = f \rho^2 (1 + 3\gamma) V^4 - \xi (\gamma - 1) W^2 / A$  and  $h(V) = -2 \rho (P_{pr_0} + \eta_e \eta_{mr} P_{ap}) V$ . It is then assumed that the exact real positive solution to the perturbed problem is expressed in terms of regular perturbation series, where the leading-order solution is obtained from the unperturbed equation  $g(V_0) = 0$ , namely

$$V_0 = \sqrt{\frac{W}{2 \rho A}} \sqrt[4]{\frac{4 \xi (\gamma - 1)}{f (1 + 3\gamma) / A}} = v_{i0} \sqrt[4]{\frac{4 \xi (\gamma - 1)}{f (1 + 3\gamma) / A}} \quad (35)$$

The approximate solution is thus sought by considering only the first-order terms of the regular perturbation series, such that  $V \approx V_0 + \epsilon V_1$ . One obtains:

$$V_1 = -\frac{P_{pr_0} + \eta_e \eta_{mr} P_{ap}}{2 f \rho (1 + 3\gamma) V_0^2} \quad (36)$$

with the result that, after restoring the artificial perturbation parameter to 1, the approximate first-order best range airspeed for a battery-powered helicopter is:

$$V_{BR} \approx V_0 \left[ 1 - \frac{P_{pr_0} + \eta_e \eta_{mr} P_{ap}}{2 f \rho (1 + 3\gamma) V_0^3} \right] \quad (37)$$

If  $\gamma = -1$ , the ideal situation in which discharge time is inversely proportional to absorbed power is recovered.<sup>6</sup> In such a particular case, the zeroth-order solution identified by equation (35) exactly matches the approximate result obtained in equation (25) for the same class of rotorcraft.

### Numerical Validation

The analytical framework proposed for cruise performance analysis and optimization is validated by means of numerical simulations for two test cases, related to different classes of rotorcraft. Results are discussed for a conventional turbine-powered medium-lift rotorcraft (hereinafter referred to as “Helicopter 1”) and for a small-scale radio controlled electric platform (referred to as “Helicopter 2”), for which fuel consumption and battery-pack model parameters are respectively provided.

#### Turbine-powered helicopter

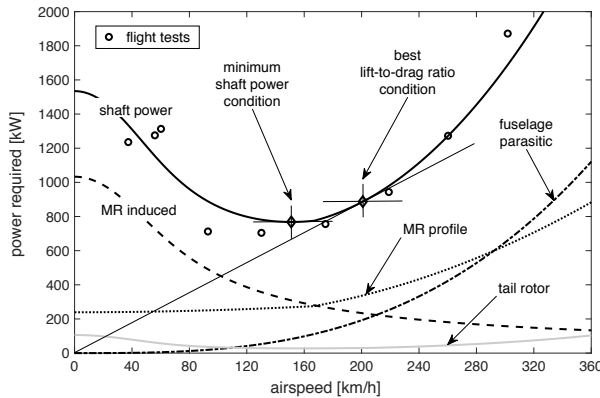
Helicopter 1 is a four-bladed, medium-lift utility helicopter powered by  $N_e = 2$  turboshaft engines. Relevant data are summarized in Table 1. Power contributions required in straight-and-level flight at different airspeeds for an operating altitude of 1585 m are detailed in Fig. 3. This plot is derived assuming that equilibrium conditions



**Table 1.** Parameters for Helicopter 1 (turbine-powered rotorcraft).

Parameter	Symbol	Value	Units
<b>Relevant aircraft data</b>			
Initial gross weight	$W_i$	71 157.1	N
Flat plate drag area	$f$	2.137	m <sup>2</sup>
Air density @ 1 585 m	$\rho$	1.0492	kg m <sup>-3</sup>
Speed of sound @ 1 585 m	$a$	334.16	m s <sup>-1</sup>
Rotor shafts distance	$l_{tr}$	9.9	m
<b>Powerplant</b>			
Number of engines	$N_e$	2	
Available fuel weight	$W_{fuel}$	9 806.6	N
Fuel flow model coefficients	$\bar{c}_0$	0.106	N s <sup>-1</sup>
	$c_1$	$4.06 \cdot 10^{-7}$	N W <sup>-1</sup> s <sup>-1</sup>
Accessory gearbox req. power	$P_{acc}$	8	kW
Main rotor transmission eff.	$\eta_{mr}$	0.9	
Tail rotor transmission eff.	$\eta_{tr}$	0.9	
<b>Main rotor (tail rotor)</b>			
Number of blades	$N_b$	4 (4)	
Radius	$R$	8.23 (1.68)	m
Chord	$c$	0.52 (0.24)	m
Solidity	$\sigma$	0.0802 (0.1852)	
Speed	$\Omega$	256.4 (1 189.3)	rpm
Blade profile drag coefficients	$C_{d0}$	0.008 (0.008)	
	$k$	0.008 (0.008)	
Induced power factor	$\xi$	1.15 (1.15)	
Drag divergence Mach number <sup>28</sup>	$M_{dd}$	0.8 (0.8)	

in equation (4) are satisfied at each airspeed for  $W = W_i$ , with a main rotor disk angle of attack equal to  $\alpha = \arcsin(-D/T)$ , provided  $T$  is given by equation (5) and tip speed is constant for both main and tail rotor. Downwash velocity at rotor disk,  $v_i$ , is obtained from equations (2) and (3) by means of a Newton-Raphson iterative scheme with 0.05%-error stop criterion.<sup>21</sup> Induced velocity at hover,  $v_{i0} = \sqrt{W_i/(2\rho A)} = 12.62$  m/s, with rotor disk area  $A = \pi R^2 = 212.8$  m<sup>2</sup>, is the starting guess value for fast convergence of the iterative scheme. The

**Figure 3.** Power required in forward flight with  $W = W_i$  (Helicopter 1, data source: Ballin<sup>29</sup>).

total shaft power required to the turbine engines decreases rapidly as speed increases from zero as a result of the drop in the induced power, reaching a minimum at  $V = V_{Pmin} = 151$  km/h. As speed increases beyond  $V_{Pmin}$ , the (increasing) contribution of airframe drag to total required power becomes predominant with respect to induced power, and the total shaft power rapidly grows with  $V$ . The resulting power estimate is consistent with available experimental data for the same helicopter,<sup>29</sup> with acceptable accuracy.

There exists a point, at a speed higher than that for minimum shaft power, where the ratio  $V/P_{sh}$  is maximized (or, equivalently, the ratio  $P_{sh}/V$  is minimized). This point is graphically determined by drawing a line passing through the origin of the axes, tangent to the  $P_{sh}$  vs  $V$  curve, as represented in Fig. 3. Letting  $P_{sh} = D_{eq} V$ , where  $D_{eq}$  can be defined as the equivalent total rotorcraft drag at a given airspeed  $V$ , the point where  $V/P_{sh}$  is maximized is representative of the best “lift-to-drag” condition,  $(L/D_{eq})_{max}$ , where “lift”  $L = T \cos \alpha$  (that is, the thrust component along the local vertical) equates aircraft weight. For  $W = W_i$  this point is located at  $V = V_{(L/D)_{max}} = 200.8$  km/h.

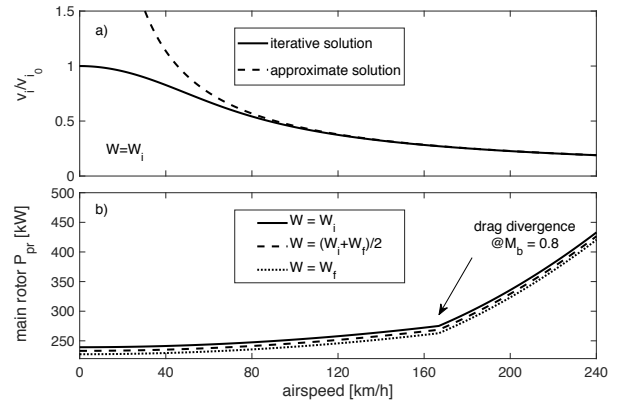
**Figure 4.** a) Downwash velocity as obtained from iterative computation and according to Assumption 1; b) main rotor profile power (Helicopter 1).

Figure 4.a shows a comparison between downwash velocity obtained by numerical computation and the approximate value determined according to Assumption 1. Results are normalized with respect to the downwash velocity at hover,  $v_{i0}$ . As  $v_i$  becomes small if compared to  $V$ , the approximation proposed in Assumption 1 appears to be reasonable, when forward speed is sufficiently high. This implies that the closed-form expressions derived for endurance and range of a turbine-powered helicopter provide accurate results only for sufficiently high forward speeds (higher than approximately 70 km/h, for Helicopter 1). On the other hand, if performance optimization is sought, best endurance and best range conditions are effectively located in the high speed range, providing a fuel-efficient cruise flight which results to be accurately identified by the obtained analytical solutions.

Figure 4.b shows the behavior of main rotor profile power as a function of forward speed, with curves parametrized in terms of aircraft gross weight. Assuming that a quantity of fuel equal to  $W_{fuel} = 9 806.6$  N is burned, corresponding to 1 000 kg, the final helicopter weight  $W_f = 61 350.4$  N is obtained. It can be noted how the variation of profile power determined by fuel consumption (which causes a 13.8% total weight loss) is less than 5% for all the considered cruise speeds, a variation which, in addition, always accounts for less than 1% of total required power. This allows one to assume that profile power does not depend significantly on actual helicopter weight during cruise flight, at any considered airspeed  $V$ . Hence, Assumption 5 is retained

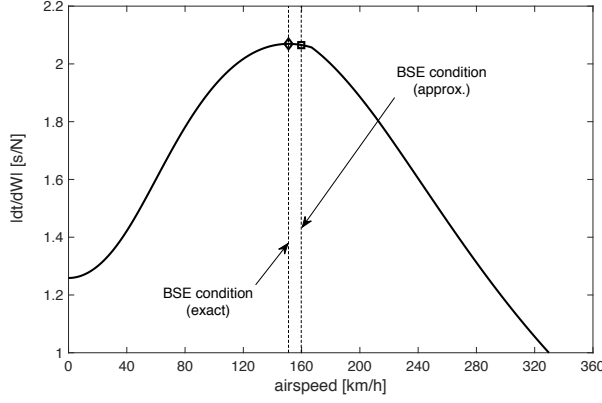


Figure 5. Specific endurance for  $W = W_i$  (Helicopter 1).

and it is possible to assume  $P_{pr} = P_{pr_i} = P_{pr}(W = W_i)$  for the analytical computation of cruise endurance and range. In Figure 4.b the onset of drag rise phenomenon is also depicted, occurring at about  $V = 167$  km/h, where the advancing blade tip Mach number equals  $M_{dd} = 0.8$ .

At the considered altitude, atmospheric pressure ratio in standard conditions is given by  $\delta = p(h)/p_{SL} = 0.8258$ , whereas temperature ratio is such that  $\theta = \Theta/\Theta_{SL} = 0.9642$  (temperature  $\Theta$  is expressed in Kelvin.<sup>21</sup>). Given  $\bar{c}_0 = 0.106$  N/s, the proposed fuel consumption model is identified by parameters  $c_0 = N_e \delta \sqrt{\theta} \bar{c}_0 = 0.171$  N/s and  $c_1 = 4.06 \cdot 10^{-7}$  N/(W s). Based on the definition in equation (12), the variation of specific endurance with  $V$  is depicted in Fig. 5, for the initial helicopter weight. The BSE condition for  $W = W_i$  is obtained by flying at the minimum shaft power speed, identified by  $V_{BSE} = V_{P_{min}} = 151$  km/h, where  $P_{sh_{min}} = 768.09$  kW and  $|dt/dW|_{max} = 2.069$  s/N (diamond marker in Fig. 5). The approximate value of BSE speed according to equation (14) is 159.75 km/h (square marker), which results into an estimate of specific endurance equal to  $|dt/dW|_{max} = 2.066$  s/N, with a +5.8% error in the determination of  $V_{BSE}$ , but only a -0.15% error for the specific endurance.

In Fig. 6 the exact endurance in steady level flight is reported for different values of airspeed (gray solid line), given the same quantity of usable fuel, as obtained from numerical integration of specific endurance by trapezoidal rule, with 0.005 kg integration step.<sup>25</sup> In the same figure, the exact specific endurance curve is reported for both the initial and the final weight (black solid lines). It is evident that, going from  $W_i$  to the final weight  $W_f$ , the BSE speed moves to a lower value, that is  $V_{BSE}(W_f) = 139.7$  km/h, providing improved punctual performance. Three constant-speed cruise programs can be thus envisaged, with the aim to obtain the best performance: 1) the helicopter is flown at constant speed  $V_{BSE}(W_i)$ , thus maximizing the specific endurance in the initial condition; 2) the helicopter is flown at constant speed  $V_{BSE}(W_f)$ , thus maximizing the specific endurance in the final condition; 3) the mission is performed at a constant speed that maximizes the overall cruise endurance, namely  $V_{BE} = 145$  km/h, such that  $t = t_{max} = 353$  min. In this latter case, cruise speed lies in between  $V_{BSE}(W_f)$  and  $V_{BSE}(W_i)$ , namely  $V_{BSE}(W_f) < V_{BE} < V_{BSE}(W_i)$ , and it is equal to the airspeed that maximizes

specific endurance at an intermediate rotorcraft weight  $W_{BSE}^* = 65969$  N  $\approx (W_i + W_f)/2$ . Hence, the exact value of best endurance airspeed  $V_{BE}$  can be determined with excellent accuracy from the value of  $V_{BSE}(W_{avg})$ , evaluated for the average weight,  $W_{avg} = (W_i + W_f)/2 = 66254$  N. For the present test case,  $V_{BSE}(W_{avg}) = 145.5$  km/h, with a difference of only +0.34% with respect to the exact value,  $V_{BE}$ . Finally, the exact endurance curve is

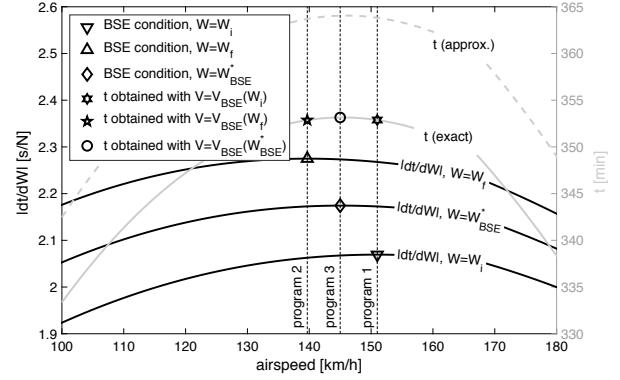


Figure 6. Endurance analysis and optimization (Helicopter 1).

compared to the one obtained by the approximate closed-form expression provided by equations (15)-(17). In this respect, the estimation error remains satisfactory for all forward speeds, reaching a maximum value of only 4.5% at the end of the considered speed range.

Based on the definition in equation (18), the exact specific range curve in the initial condition is reported in Fig. 7 as a function of forward speed  $V$ . The BSR speed for  $W = W_i$  is exactly identified by  $V_{BSR} = 229$  km/h, where  $P_{sh_{BSR}} = 1039.9$  kW and  $|dx/dW|_{max} = 107.2$  m/N (diamond marker in Fig. 7). The approximate value to the BSR speed according to equation (22) is 237.3 km/h, with about +3.6% estimation error (square marker). The corresponding approximate value of the BSR is  $|dx/dW|_{max} = 107$  m/N, which results into an estimation error smaller than -0.2%. The zeroth-order approximation provided by equation (25) coincides with the solution obtained by Leishman,<sup>21</sup> with a BSR airspeed of 210.2 km/h, which underestimates the exact value by as much as 8.2%

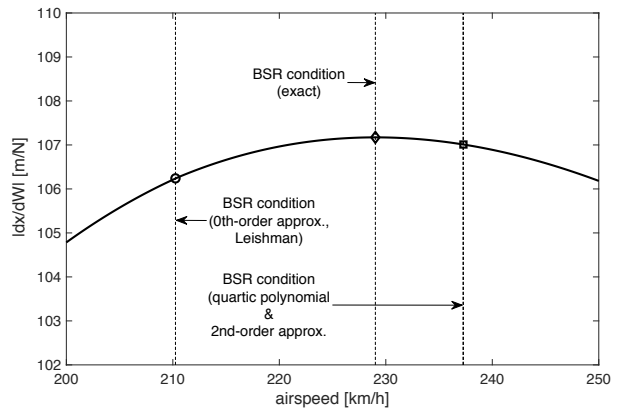


Figure 7. Specific range for  $W = W_i$  (Helicopter 1).

(circle marker). The best specific range estimate exactly at this point is 106.2 m/N, with an error in the order of  $-0.9\%$ . Finally, the approximate value obtained in equation (28) as a second-order perturbation to the zeroth-order solution is 237.2 km/h (practically equal to the value obtained by equation (22)), with about  $+3.6\%$  speed estimation error, and a corresponding underestimate of best specific range by about  $-0.2\%$ .

Fig. 8 depicts the distance flown in steady level flight for different values of airspeed and the given amount of usable fuel, as obtained from numerical integration of specific range (gray solid line). In the same figure, the exact specific range curve is also reported for both the initial and the final weight configurations (black solid lines). As for flight endurance, the speed that maximizes the overall cruise range,  $V_{BR} = 225$  km/h, lies in between  $V_{BSR}(W_f) = 219.9$  km/h and  $V_{BSR}(W_i) = 229$  km/h, that is  $V_{BSR}(W_f) < V_{BR} < V_{BSR}(W_i)$ , and it is equivalent to the speed that would maximize the specific endurance for an intermediate rotorcraft weight  $W_{BSE}^* = 66\,842$  N  $\approx (W_i + W_f)/2$ . Once again,  $V_{BR}$  can be well approximated by evaluating  $V_{BSR}(W_{avg}) = 224.5$  km/h, with an error equal to about  $-0.2\%$  with respect to  $V_{BR}$ .

Finally, the exact range curve is compared to that obtained by the approximate closed-form expression provided in equations (16), (17), and (29). Note that the exact range curve is fairly flat near  $V_{BR}$ , such that flying at speeds different than  $V_{BR}$  does not result into significant performance degradation. For example, the cruise range obtained by flying at 210.2 km/h (BSR speed for  $W = W_i$ , according to the best range solution derived by Leishman<sup>21</sup>) is equal to 1070.4 km. When flying at 237.2 km/h (that is, the BSR speed for  $W = W_i$ , according to the proposed second-order approximation in equation (28)), a range of about 1072.4 km is obtained, which is only 0.2% bigger than the former value. In this latter case, however, the helicopter is flying at a higher speed, such that the considered cruise mission can be completed with a significant reduction of required flight time (about 34 min, corresponding to  $-11.2\%$ ). In view of this consideration, it is evident that a more accurate estimation of best range speed with respect to the (underestimated) results proposed in literature, allows one to improve the overall mission and performance capabilities.

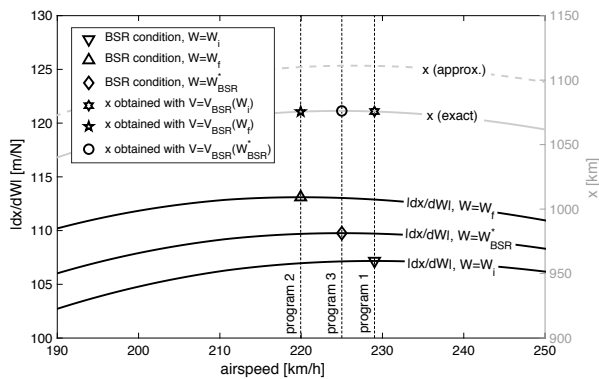


Figure 8. Range analysis and optimization (Helicopter 1).

Table 2. Parameters for Helicopter 2 (battery-powered rotorcraft).

Parameter	Symbol	Value	Units
<i>Relevant aircraft data</i>			
Weight	$W$	28.44	N
Flat plate drag area	$f$	0.014	m <sup>2</sup>
Air density @ 100 m	$\rho$	1.2133	kg m <sup>-3</sup>
Rotor shafts distance	$l_{tr}$	0.68	m
<i>Powerplant</i>			
Number of engines	$N_e$	1	
Battery nominal capacity	$C_0$	5	A h
Battery model coefficients	$\lambda$	24.95	
	$\gamma$	-1.021	
	$\beta$	0.9664	
Avionics and payload req. power	$P_{ap}$	6	W
Electric systems eff.	$\eta_e$	0.75	
Main rotor transmission eff.	$\eta_{mr}$	0.92	
Tail rotor transmission eff.	$\eta_{tr}$	0.9	
<i>Main rotor (tail rotor)</i>			
Number of blades	$N_b$	2 (2)	
Radius	$R$	0.57 (0.12)	m
Chord	$c$	0.036 (0.024)	m
Solidity	$\sigma$	0.0402 (0.1273)	
Speed	$\Omega$	2200 (9900)	rpm
Blade profile drag coefficients	$C_{d0}$	0.008 (0.008)	
	$k$	0.008 (0.008)	
Induced power factor	$\xi$	1.2 (1.2)	

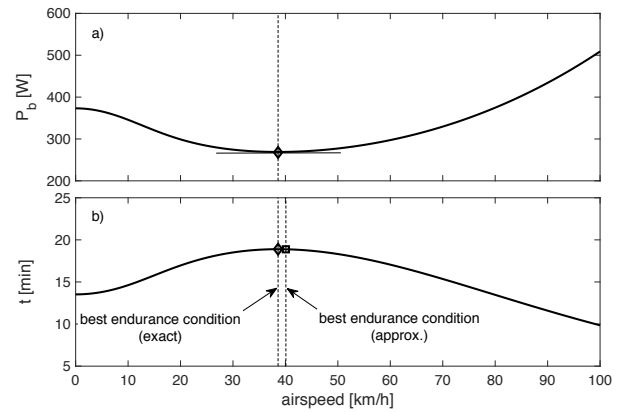


Figure 9. a) Battery power required in straight-and-level flight; b) cruise endurance (Helicopter 2).

### Battery-powered helicopter

Helicopter 2 is a two-bladed, small-scale radio-controlled helicopter powered by a brushless high-speed electric motor. Relevant data are summarized in Table 2, including the parameters necessary to identify the constant power battery-discharge model.<sup>6</sup> In particular, a battery pack made of a series connection of 6 Lithium-Polymer cells is discharged to the 80% of nominal capacity  $C_0 = 5$  Ah, such that  $C = 0.8 C_0 = 4$  Ah.

The total battery power required for Helicopter 2 in straight-and-level flight at an operating altitude of 100 m is reported in Fig. 9.a. Please note that compressibility effects are not included in the model of Helicopter 2, given the expected flight envelope of a small size electrical helicopter. Again, downwash velocity,  $v_i$ , is obtained by means of Newton-Raphson iterative approach, provided that the value at hover is  $v_{i0} = \sqrt{W/(2\rho A)} = 3.39$  m/s, where  $A = \pi R^2 = 1.02$  m<sup>2</sup>. In Fig. 9.b the exact endurance is reported as a function of airspeed. Provided that vehicle weight

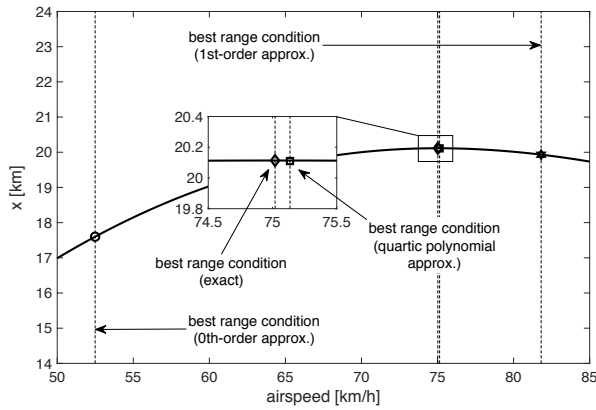


Figure 10. Cruise range (Helicopter 2).

is now constant (no fuel is burned and battery weight is independent of the state of charge), best endurance is simply obtained by maximizing battery discharge time, flying at the minimum required power condition, which is exactly identified by  $V_{BE} = V_{P_{min}} = 38.60$  km/h, with  $P_{b_{min}} = 267.82$  W, and  $t_{max} = 19$  min (diamond marker). Taking into account Assumptions 1-4, the approximate value of best endurance airspeed according to equation (14) is 40.09 km/h, which overestimates the exact value by +3.9% (square marker).

The range available flying at different airspeed, calculated according to equation (33), is plotted in Fig. 10. Best range speed is  $V_{BR} = 75.46$  km/h, where  $V P_b^\gamma$  is maximized, with  $P_{b_{BR}} = 352.54$  W, and  $x_{max} = 18.03$  km (diamond marker). The approximate value to best range airspeed according to equation (22), adapted to the case of a (constant weight) battery-powered helicopter, is 75.14 km/h, with a -0.4% error (square marker in the zoomed figure view). The zeroth-order approximation in equation (35) gives 52.49 km/h, underestimating the exact value by more than 30% (circle marker). Finally, the approximate value obtained from equation (37) as a first-order perturbation to the zeroth-order solution is 81.81 km/h, overestimating  $V_{BR}$  by only 8.4% (hexagon marker).

## Conclusions

Range and endurance performance of turbine-powered conventional helicopters in forward flight is analyzed. Best endurance and best range conditions are derived in terms of cruise airspeed and compared to long-standing results available in literature. A reasonably accurate model for engine specific fuel consumption is introduced, easily adapted to the case of piston engine rotorcraft. When rotor profile power, main rotor induced power and parasitic power contributions are accounted for, a fully analytical framework is derived, which provides results more accurate than those obtained from available methods. Closed-form expressions are obtained for both endurance and range of a constant speed cruise and a given amount of usable fuel.

The resulting performance analysis tools are at one time simple and of general validity, easily extended to the case of battery-powered helicopters. To this aim, a recent model for battery discharge time during a constant-power discharge

process is adopted. The approach is quantitatively validated by means of two test cases, namely a medium-lift utility helicopter powered by two turboshaft engines and a small scale battery-powered rotorcraft. Results are compared with those available in the literature, showing that more accurate results can be obtained, with closed-form expressions which depend on a limited set of relevant system parameters.

## References

1. Von Mises R. *Theory of Flight*. New York: McGraw-Hill Book Co. Inc., 1945, pp. 463-465.
2. Austyn Mair W and Birdsall DL. *Aircraft Performance*. Cambridge: Aerospace Series, Vol. 5, Cambridge University Press, 1998, pp. 166-169.
3. Anderson JD. *Aircraft Performance and Design*. 1st ed. New York: McGraw-Hill Higher Education, 1999, pp. 293-316.
4. Traub LW. Range and Endurance Estimates for Battery-Powered Aircraft. *J Aircr* 2011; 48(2):703-707.
5. Avanzini G and Giulietti F. Maximum Range for Battery-Powered Aircraft. *J Aircr* 2013; 50(1):304-307.
6. Avanzini G, de Angelis EL and Giulietti F. Optimal performance and sizing of a battery-powered aircraft. *Aerosp Sci Technol* 2016;59:132-144.
7. Ferguson K and Thomson D. Performance comparison between a conventional helicopter and compound helicopter configurations. *Proc IMechE Part G: J Aerospace Engineering* 2015; 229(13):2441-2456.
8. Han D, Pastrikakis V and Barakos GN. Helicopter performance improvement by variable rotor speed and variable blade twist. *Aerosp Sci Technol* 2016; 54:164-173.
9. Han D, Yang K, and Barakos GN. Extendable chord for improved helicopter rotor performance. *Aerosp Sci Technol* 2018; 80:445-451.
10. Wang Q and Zhao Q. Rotor blade aerodynamic shape optimization based on high-efficient optimization method. *Proc IMechE Part G: J Aerospace Engineering* 2019; 234(2):375-387.
11. Lu Y, Su T, Chen R, et al. A method for optimizing the aerodynamic layout of a helicopter that reduces the effects of aerodynamic interaction. *Aerosp Sci Technol* 2019; 88:73-83.
12. Misté GA and Benini E. Variable-Speed Rotor Helicopters: Performance Comparison Between Continuously Variable and Fixed-Ratio Transmissions. *J Aircr* 2016; 53(5):1-12.
13. Siva C, Murugan MS and Ganguli R. Uncertainty Quantification in Helicopter Performance Using Monte Carlo Simulations. *J Aircr* 2011; 48(5):1503-1511.
14. Visser HG. Optimization of Balanced Field Length Performance of Multi-Engine Helicopters. *J Aircr* 2000; 37(4):598-605.
15. de Angelis E. Stability analysis of a multicopter vehicle hovering condition. *Aerosp Sci Technol* 2018; 72:248-255.
16. Jin Y, Yong L and Weidong Y. Dynamics research on actively controlled swashplateless rotor. *Proc IMechE Part G: J Aerospace Engineering* 2019; 233(12):4492-4508.
17. Abhiram DR, Ganguli R, Harursampath D, et al. Robust Design of Small Unmanned Helicopter for Hover Performance Using Taguchi Method. *J Aircr* 2018; 55(4):1745-1752.
18. Hu Y and Rao SS. Robust Design of Horizontal Axis Wind Turbines Using Taguchi Method. *J Mechanical Design* 2011; 133(11):1-15.

19. Shrestha R, Benedict M, Hrishikeshavan V, et al. Hover Performance of a Small-Scale Helicopter Rotor for Flying on Mars. *J Aircr* 2016; 53(4):1160-1167.
20. Johnson W. *Helicopter Theory*. New York: Dover Publications, Inc., 1994, pp. 299-300.
21. Leishman JG. *Principles of Helicopter Aerodynamics*. 2nd ed. New York: Cambridge University Press, 2006, Chs. 2 and 5.
22. McCormick BW. *Aerodynamics, Aeronautics, and Flight Mechanics*. 2nd ed. New York: John Wiley & Sons, Inc., 1994, pp. 413-419.
23. Stepniewski WZ and Keys CN. *Rotary-Wing Aerodynamics*. New York: Dover Publications, Pt. 2, 1984, Chs. 2 and 3.
24. Brent RP. *Algorithms for Minimization Without Derivatives*. 1st ed. Prentice-Hall, Upper Saddle River, 2013, Ch. 5.
25. Press WH, Teukolsky SA, Vetterling WT, et al. *Numerical Recipes: The Art of Scientific Computing*. 3rd ed. Cambridge: University Press, 2007, Chs. 4 and 10.
26. Rees EL. Graphical Discussion of the Roots of a Quartic Equation. *The American Mathematical Monthly* 1922; 29(2):51-55.
27. Kokotović P, Khalil HK and O'Reilly J. *Singular Perturbation Methods in Control: Analysis and Design*. Philadelphia: Society for Industrial and Applied Mathematics, 1999, Ch. 1.
28. Totah J. *A Critical Assessment of UH-60 Main Rotor Blade Airfoil Data*. NASA Technical Memorandum 103985, 1993, Appendix.
29. Ballin MG. *Validation of a real-time engineering simulation of the UH-60A helicopter*. NASA Technical Memorandum 88360, 1987, Appendix B.